# An exergoeconomic and normalized sensitivity based comprehensive investigation of a hybrid power-and-water desalination system

Muhammad Ahmad Jamil[a♣], Haseeb Yaqoob[b,c], Asad Abid[b], Muhammad Umer Farooq[b], Noor us Sabah[b], Ben Bin Xu[a], Laurent Dala[a], Kim Choon Ng[d], Muhammad Wakil Shahzad[a♣]

[a]Mechanical & Construction Engineering Department, Northumbria University, Newcastle Upon Tyne, NE1 8ST UK
[b]Department of Mechanical Engineering, Khwaja Fareed University of Engineering and Information Technology, Rahim Yar Khan 64200, Pakistan
[c]School of Mechanical Engineering, Engineering Campus, Universiti Sains Malaysia, Nibong Tebal 14300, Penang, Malaysia
[d]Water Desalination and Reuse Centre, King Abdullah University of Science & Technology, 23955-6900 Thuwal, Saudi Arabia

## ABSTRACT

Cogeneration of power-and-water is one of the potential solutions for ever-rising energy and freshwater demand. These systems have shown superior thermodynamic and economic performance compared to their standalone counterparts because of processes synergy and shared utilities resources. The current study investigates a multi-effect distillation system operated on bleed-out steam from the last stages of low-pressure steam turbine of a combined cycle gas turbine power plant (CCGT+MED). For this purpose, a component-based exergoeconomic investigation integrated with normalized sensitivity analysis for energy, exergy, and economic evaluation. The performance indicators include specific fuel consumption, thermal efficiency, exergy destruction, exergy efficiency, stream cost, and product cost (electricity and freshwater). The analysis showed that the cogeneration scheme reduced the electricity cost by 16.8% and freshwater production cost by 24.5% compared to the standalone power plant and MED systems. Moreover, the payback period for the MED system is calculated as 2.59 years with freshwater selling at \$1.6 /$m^3$. The sensitivity analysis showed that the electricity and the freshwater production cost are the most sensitive to gas turbine efficiency, fuel cost, and fuel heating value with normalized sensitivity coefficients of 1.71, 0.86, and 0.80 for electricity and 0.76, 0.42 and 0.40, for freshwater cost, respectively. While the other parameters such as interest rate, cost index factor, steam turbine efficiencies etc. showed a remarkably low impact on the cost of the products.

**Keywords**: Multi-effect desalination, exergoeconomic analysis, water-and-power cycle, normalized sensitivity analysis

♣ Corresponding authors: muhammad2.ahmad@northumbria.ac.uk, muhammad.w.shahzad@northumbria.ac.uk

## Highlights

- Paper presents exergoeconomic and sensitivity analyses of a CCGT+MED system
- The proposed system had lower electricity and freshwater cost by 16% and 24%
- Electricity and freshwater costs are \$0.033-0.089/kWhr and \$1.2-2.41\$/$m^3$
- The payback period of system is 2.59 years with freshwater selling
- Electricity and water costs are sensitive to turbine efficiency and fuel cost

## 1. Introduction

Water and energy are among the major challenges faced globally because of a growing population, depletion of conventional sources, and high carbon footprints [1,2]. Therefore, it is needful to maintain a sustainable nexus between water, energy, and the environment for an economical lifestyle [3,4]. Unfortunately, the global water scarcity is expected to surpass 4000 billion cubic meters per year ($Bm^3$/year) by 2030 resulting in a water shortage problem for more than 5 billion people worldwide [5,6]. In this regard, desalination has been proven a viable option to ameliorate the water supply-demand gap [7]. Therefore, a significant increase in the installed desalination capacity has been observed over the years and is predicted to expand further in the future as shown in Figure 1 [8,9]. Meanwhile, besides augmenting the installed capacity, the improvements in existing system performance have also been focused [10,11]. Some of the latest developments include hybridization of cycles [12,13], integration of energy recovery [14,15], innovative technologies [16,17] and developments of renewable energy-based systems [18,19].

However, despite significant efforts, the specific derived energy consumption of conventional commercial-scale technologies is still very high as; reverse osmosis (RO) 3.7-8 kWh/$m^3$ electric, multi-effect distillation (MED) 7-21 kWh/$m^3$, multi-stage flash (MSF) 19-27 kWh/$m^3$, mechanical vapor compression system (MVC) 7-12 kWh/$m^3$, and thermal vapor compression (TVC) 12-16 kWh/$m^3$ [20]. On the other hand, the minimum separation work for desalination at infinitesimal recovery is estimated as 0.72 kWh/$m^3$ for a salinity of 35 g/kg (feed) at 25 °C [21,22]. It shows that the conventional technologies are energy-intensive and operate only at 10-13% of their thermodynamic limit [23]. Therefore, a significant research gap still exists for energy efficiency improvement of existing desalination systems [24]. In this regard, the cogeneration of the power-and-water cycle is one of the lucrative options to achieve high thermodynamic efficiency and low water and power production costs [25]. In this scheme, a desalination system is coupled with a

combined cycle gas turbine (CCGT) power plant for simultaneous power-and-water production [26]. It has shown several benefits like lower condenser water and area, low thermal losses, lesser fuel consumption, and reduction in operational expenses (due to sharing of facilities i.e., preheated feed, fuel, and labor, etc.) [27,28].

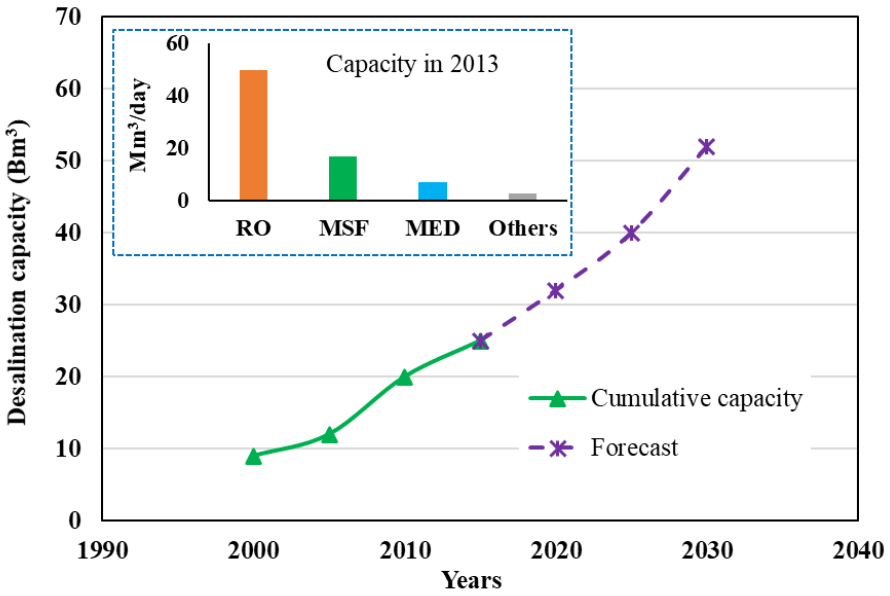


**Figure 1.** Global desalination trend and prediction [8,9].

Owing to the above-mentioned advantages and potential to outperform the stand-alone desalination systems, significant efforts have been made to enhance the performance of cogeneration systems recently. For instance, Ghorbani et al. [29] proposed a novel phase change material-assisted solar-based steam power plant (1063 MW) integrated with a multi-effect desalination system that produced 8321 kg/s of freshwater using 2571MW of waste heat. They reported the electrical, thermal, and exergy efficiencies for the hybrid system as 28.84%, 97.18%, and 52.23% respectively. Mohammadi et al. [30] analyzed the feasibility of different trigeneration systems for the production of electricity, freshwater, and cooling using CCGT. They reported the Levelized costs of electricity, water, and cooling to be ranging from \$0.06598-0.06428/kWh, \$1.146-1.575/$m^3$, \$0.0389-0.0930/ton-hr, respectively for CCGT + double-effect absorption chiller + MED. Lee and Park [31] proposed a novel cogeneration plant based on liquefied natural gas (LNG) cold energy. They reported the specific energy consumption and the product cost for the proposed system as 5.202 kWh/ton and \$0.148/ton of pure water which are lower than the conventional systems. Abdulrahim and Chung [32] studied the effect of intake air cooling in a

cogeneration plant during summer conditions using an evaporative cooler (EC) and absorption refrigerator (AR) in two different scenarios. They reported around 5.89% and 9.11% increase in the energy utilization factor of the plant by EC and AR, respectively.

Besides, Sorgulu and Dincer [33] proposed a biomass-based cogeneration system for electricity and freshwater production as well as waste minimization. The system used 2.498 kg/s of municipal solid waste and 0.1314 kg/s of olive oil waste to produced 4.49 MW of electricity using a steam turbine and 92.29 kg/s of freshwater through MED and RO systems. They reported the overall energy and exergy efficiencies as 37.04% and 19.78%, respectively. Ding et al. [34] optimized a gas turbine cycle integrated with Kalina + HDH cycles as the waste heat recovery systems for water and power production. The maximum exergy efficiency and minimum value of Levelized total emission were calculated as 43.84% and 62602 kg/kW, respectively. Delpisheh et al. [35] proposed a novel solar-assisted freshwater and hydrogen cogeneration system. The cycle's waste heat was used to produce fresh water using a humidification dehumidification desalination system. The maximum exergy efficiency and unit exergy cost of the proposed system was reported as 5.39% and 81.4 $/GJ, respectively. Similarly, some other cogeneration options are integration with nuclear power plants [36], algal cultivation systems [37], and solar-based regeneration systems [38], etc.

The above review suggests that the cogeneration water-and-power scheme offers several benefits like lower energy consumption, high thermodynamic performance, and lower energy and water production cost compared to the standalone systems. Therefore, the current study presents a comprehensive analysis of a combined cycle gas turbine integrated multi-effect desalination system (CCGT+MED). For this purpose, two important system analysis methods including component-based exergoeconomic analysis and an advanced Normalized Sensitivity Analysis (NSA) are used. The first is employed as a combined application of thermodynamic and economic analyses which allows a separate audit of each component in the system to assess how efficiently it utilizes the supplies. The second one (i.e., NSA) is used for one-on-one comparison of different parameters with significantly different magnitude to identify the most influential ones. These methods allow a closer insight into the plant performance than the conventional thermodynamic, economic, and parametric analyses which rely on overall system performance analysis based on the resources invested at system boundaries. The analysis is focused on energy, exergy, and economic viewpoints estimating fuel consumption, exergy destruction, capital investment, stream cost, payback period, and parametric analyses.

## 2. System description

A forward feed multi-effect desalination system (MED) integrated with a combined cycle gas turbine (CCGT) power plant is considered for the study. The CCGT consists of a single-stage gas turbine and three stages steam turbines i.e., high pressure (HP), medium pressure (MP), and low pressure (LP)) with a total power output of 592.2 MW. While the MED system consists of 6 evaporators (N=6) with a total water production capacity of 50 kg/s. Figure 2 presents the schematic diagram for considered CCGT+MED systems with a description of each point. It is important to mention that, the plant layout and process parameters are considered from a recent study by Shahzad et al. [39]. The process starts, as the waste heat (flue gases) from the gas turbine outlet, is used in a heat recovery steam generator (HRSG) to produce steam. The steam is first fed to the high-pressure stage of the steam turbine from where it is directed to the medium pressure after being reheated in HRSG and finally to the low-pressure stage. From the low-pressure stage, the steam is bled to the MED system as a heat source in the first evaporator and the flow rate of bled steam is controlled by the desalination capacity of the MED system. The extra steam is condensed in a condenser using cooling water which is discarded back to the sea and condensed water is fed to the HRSG section for the next cycle. The process parameters (pressure, temperature, specific enthalpy, mass flow rate, and specific entropy) for different state points mentioned in the schematic diagram are presented in Table 1.

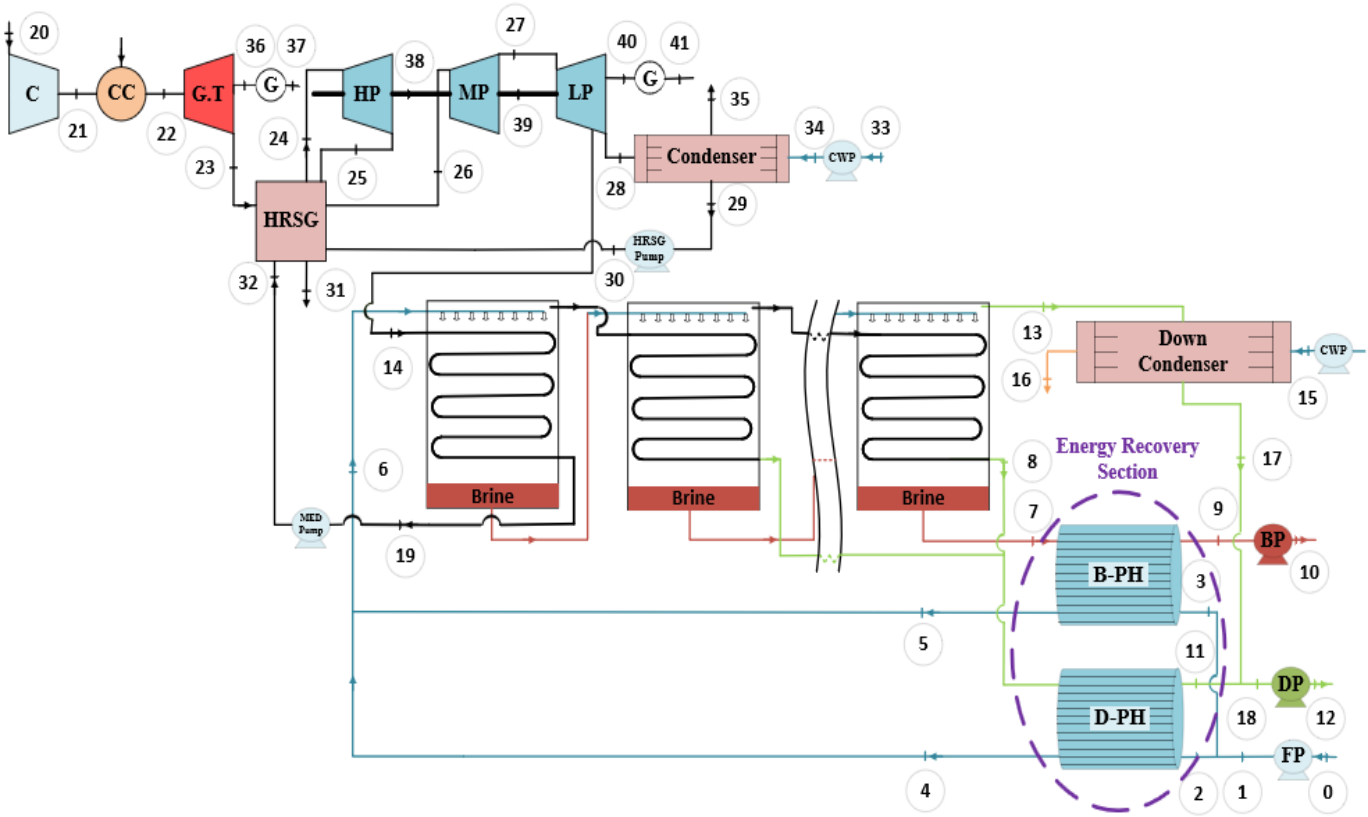


132

0. Feed to feed pump
1. Feed pump outlet
2. Feed to distillate Preheater
3. Feed to brine preheater
4. Feed from distillate preheater
5. Feed from brine preheater
6. Feed of first evaporator
7. Last effect brine into brine preheater
8. Condensate into distillate preheater
9. Brine outlet from brine preheater
10. Brine pump outlet
11. Distillate outlet from distillate preheater
12. Distillate from distillate pump outlet
13. Last effect vapors to condenser
14. Bleed steam from LP turbine
15. Cooling water to down condenser
16. Cooling water out
17. Condensate from down condenser
18. Total distillate
19. Steam condensate
20. Compressor air inlet
21. Compressed air outlet
22. Combustor chamber outlet
23. Gas turbine outlet / HRSG inlet
24. HP turbine inlet
25. HP turbine steam out
26. MP turbine inlet
27. LP turbine inlet
28. LP turbine outlet & inlet to condenser
29. Condenser outlet
30. Inlet cooling water to HRSG
31. HRSG outlet
32. Steam condensate to HRSG
33. Cooling water pump inlet
34. Cooling water to PP condenser
35. Cooling water outlet
36. Gas turbine outlet
37. Gas turbine generator outlet
38. HP turbine out
39. MP turbine out
40. LP turbine out
41. LP turbine generator out

133

134 **Figure 2.** Schematic diagram of water-and-power cogeneration scheme.

**Table 1.**

Process parameters for states points in CCGT+MED plant of Figure 2.

| State points | T (°C) | ṁ (kg/s) | P (kPa) | h (kJ/kg) | s (kJ/kg K) |
|---|---|---|---|---|---|
| 20 | 30 | 768.7 | 101.3 | 303.5 | 5.712 |
| 21 | 319 | 768.7 | 800 | 599.2 | 5.801 |
| 22 | 1197 | 1025 | 800 | 1601 | 6.827 |
| 23 | 638 | 1025 | 120 | 946.1 | 6.813 |
| 24 | 560 | 224.4 | 11300 | 3513 | 6.721 |
| 25 | 380 | 224.4 | 2800 | 3189 | 6.891 |
| 26 | 560 | 224.4 | 2800 | 3594 | 7.438 |
| 27 | 310 | 224.4 | 1000 | 3072 | 7.162 |
| 28 | 46 | 209.1 | 10 | 2584 | 8.145 |
| 29 | 37 | 209.1 | 8.83 | 2568 | 0.532 |
| 30 | 37 | 209.1 | 78.83 | 155 | 0.532 |
| 31 | 97 | 1025 | 120 | 371 | 7.03 |
| 32 | 71.5 | 15.28 | 220 | 299.4 | 0.9731 |
| 33 | 22.5 | 39.33 | 101 | 94.47 | 0.3162 |
| 34 | 22.5 | 39.33 | 151 | 94.51 | 0.3612 |
| 35 | 43 | 39.33 | 131 | 180.2 | 0.5844 |

## 3. Mathematical model

### *3.1. Thermodynamic analysis*

The thermodynamic analysis involves the calculation of energy consumed, produced, or transformed during operation. For instance, work input to the compressor, heat supplied in the combustion chamber, work produced by turbines, energy interaction in heat recovery steam generation system, and thermodynamic efficiency of the plant. The governing equations for different components in the systems are presented in Table 2 and the numeric subscripts correspond to different states in the system as illustrated in Figure 2. It is important to mention that the thermophysical properties i.e., specific heats, enthalpies, entropies, etc. used in the mathematical model for different fluid streams are not constant. Rather these are calculated using the Engineering Equation Solver (EES) built-in routines for thermophysical properties of fluids as a function of temperature and pressure for air, steam, and water streams. While for saline water, these are calculated as a function of temperature and salinity using correlations provided by [40] in the seawater library. Similarly, for flue gases, specific heat is calculated using the correlation provided in Table 2 as a function of temperature. Moreover, these properties in each case correspond to the values at an average temperature of inlet and outlet states, and different streams in the cycle are treated as follows: 20, 21 (air), 24-28 (steam), 29,30,32 (water), 33, 35 (saline/seawater), and 22, 23, 31 (flue gas). Meanwhile, it is also important to note, the work produced by the low-pressure steam turbine (refer Eq. 8) is calculated as the sum of work produced due to actual expansion of the steam and the energy that could have been produced by expanding the bleed out steam (i.e., supplied to MED). Besides, the pump work in the condenser and MED section (though very low) is taken from the steam turbine output while calculating the net work output. While the total work produced by the system is calculated as the summation of individual turbine works which after adjustment with generator efficiency represents the total electricity production capacity.

The numerical analysis is based on the following standard assumptions:(a) the intake seawater properties are $P_0$ = 101.325 kPa, $T_0$ = 22.5 $^oC$, and $S_0$ = 35 g/kg, (b) steady-state process, (c) identical heat transfer area for all evaporators, (d) the thermophysical properties are pressure, temperature and chemical composition dependent, (e) non negligible BPE effects, (f) the fuel used in the power plant is methane (g) the isentropic efficiencies for turbines are as follows: GT 83%, HPST 77%, MPST 73%, and LPST 48% [41] (h) the intake air cost at compressor inlet is zero i.e., $C_{20}$ = 0 \$/s.

**Table 2.**

Thermodynamic model of the power-desalting cogeneration scheme.

| Equipment | Governing equation | Eq. # |
|---|---|---|
| Compressor | $\dot{W}_{comp} = m_{20} Cp_{20} \left(T_{21} - T_{20}\right)$ | (1) |
| Combustion chamber [42] | $\dot{Q}_{comb,in} = LHV\,\dot{m}_f + m_{21} h_{21}$, $\dot{Q}_{comb,out} = m_{22} Cp_g \left(T_{22} - T_{21}\right)$ <br> $LHV = 47230\,kJ/kg \rightarrow \dot{Q}_{comb,in} = 1033\,MJ/s$ | (2) |
| Gas turbine [42] | $\dot{W}_{GT} = m_{22}\, Cp_g \left(T_{22}\right) \eta_{GT} \left(1 - 1/\left(P_{22}/P_{23}\right)\right)^{\frac{1.33-1}{1.33}}$ <br> $Cp_g = 0.992 + 6.99\times10^{-5}\left(T_i(K)\right) + 2.71\times10^{-7}\left(T_i(K)\right)^2$ <br> $-1.22\times10^{-10}\left(T_i(K)\right)^3$ (flue gases) | (3) |
| Heat recovery steam generation system, HRSG | $\dot{Q}_{HRSG,in} = \left(m_{23} h_{23}\right) + \left(m_{25} h_{25}\right) + \left(m_{30} h_{30}\right) + \left(m_{32} h_{32}\right)$ | (4) |
| | $\dot{Q}_{HRSG,out} = \left[m_{24}\left(h_{24} - h_{30} - h_{32}\right)\right] + \left[m_{26}\left(h_{26} - h_{25}\right)\right]$ | (5) |
| Steam turbine [25] | $\dot{W}_{HPST} = m_{24}\left(h_{24} - h_{25}\right)\eta_{HST}$ | (6) |
| | $\dot{W}_{MPST} = m_{26}\left(h_{26} - h_{27}\right)\eta_{MST}$ | (7) |
| | $\dot{W}_{LPST} = \left[m_{28}\left(h_{27} - h_{28}\right) + m_{14}\left(h_{27} - h_{14}\right)\right]\eta_{LPST}$ | (8) |
| | $\dot{W}_{ST} = \left(\dot{W}_{HPST} + \dot{W}_{MPST} + \dot{W}_{LPST}\right)\eta_{Gen}$ | (9) |
| Thermal efficiency | $\eta_{th} = \left(\dot{W}_{net,ST} + \dot{W}_{net,GT}\right)/\dot{Q}_{comb}$ | (10) |
| Exergetic efficiency | $\eta_{exergetic} = \left(\dot{W}_{net,ST} + \dot{W}_{net,GT}\right)/\left(X_{22} - X_{31}\right)$ | (11) |

### 3.2. *Exergoeconomic analysis*

Followed by energy analysis, the exergoeconomic analysis involves the computation of exergy, capital cost, and stream cost. In the first step, the exergy at each state point is calculated using mass flow rate, temperature, pressure, and chemical potential. This is followed by the calculation of stream cost using exergy, unit energy cost, and equipment purchasing cost. The operation and maintenance costs are accommodated within the fixed cost terms in the whole analysis of CCGT for which the correlations are presented in Table 3 and Table 4. For this purpose, the purchasing cost ($) is first transformed into cost rate ($/s) using availability factor, interest rate, and component life (combinedly know as capital recovery factor CRF) as given below [43].

$$\dot{Z} = \frac{Z \times CRF}{\left(365 \times 24 \times 3600 \times A\right)} \tag{12}$$

$$CRF = \frac{i\left(1+i\right)^{t}}{\left(1+i\right)^{t} - 1} \tag{13}$$

Where CRF is the capital recovery factor, $A$ is the component availability, $i$ is the interest rate, and $t$ is the plant life for which the values are summarized in Table 5 [44].

**Table 3.**
Correlations for capital cost.

| Component | Equation | Ref. |
|---|---|---|
| Pump | $Z_{Pump} = 32 \times 0.435 \times \dot{m}_{water}^{\,0.55}\, \Delta P^{0.55} \left(\frac{\eta}{\eta - 1}\right)^{1.05}$ | [57] |
| MED effect | $Z_{EV} = 201.67 \times UA_{Evap.}\, \Delta P_t^{0.15}\, \Delta P_s^{-0.15}$ | [57] |
| Preheater | $Z_{PH} = 1000\left(12.86 + A_{HT}^{0.8}\right)$ | [58] |
| Condenser | $Z_{Condenser} = 430 \times 0.582 UA_{Condenser}\, \Delta P_t^{-0.01}\, \Delta P_s^{-0.01}$ | [57] |
| Steam cost | $C_{Steam,Annual} = \frac{\left(1.466 \times h_{fg,steam} \times Availability \times 365 \times \dot{V}_{destillate}\right)}{1000 \times GOR}$ | [59] |

**Table 4.**
Correlations for the fixed cost of CCGT components.

| Component | Equation | Ref. |
|---|---|---|
| Compressor | $Z_{comp.} = C_{Comp,1} \times m_{20} \times \left( \frac{1}{C_{Comp,2} - \eta_{comp.}} \right) \times \left( P_{21} / P_{20} \right) \times \ln \left( P_{21} / P_{20} \right)$ | |
| Combustion chamber | $Z_{comb.} = C_{Comb,1} \times m_{21} \times \left( 1 + e^{C_{Comb,2} \times \left( T_{22} - C_{Comb,3} \right)} \right) \times \left( \frac{1}{0.995 - P_{22} / P_{21}} \right)$ | [61] |
| Gas turbine | $Z_{GT} = C_{\mathrm{GT},1} \times m_{22} \times \left( \frac{1}{C_{\mathrm{GT},2} - \eta_{GT}} \right) \times \ln \left( P_{22} / P_{23} \right) \left( 1 + e^{C_{\mathrm{GT},3} \times \left( T_{22} - 1570 \right)} \right)$ | |
| Steam turbine | $Z_{ST} = Z_{HPST} + Z_{MPST} + Z_{LPST}$ | [61–63] |
| | $Z_{HPST} = C_{ST} \times \dot{W}_{HPST}^{\ 0.7} \times \left( 1 + \left( \left( 1 - \eta_{HPST,1} \right) / \left( 1 - \eta_{HPST} \right) \right)^3 \right) \times \left( 1 + 5^{\left( T_{24} - 866 \right) / 10.42} \right)$ | |
| | $Z_{MPST} = C_{ST} \times \dot{W}_{MPST}^{\ 0.7} \times \left( 1 + \left( \left( 1 - \eta_{MPST,1} \right) / \left( 1 - \eta_{MPST} \right) \right)^3 \right) \times \left( 1 + 5^{\left( T_{26} - 866 \right) / 10.42} \right)$ | |
| | $Z_{LPST} = C_{ST} \times \dot{W}_{LPST}^{\ 0.7} \times \left( 1 + \left( \left( 1 - \eta_{LPST,1} \right) / \left( 1 - \eta_{LPST} \right) \right)^3 \right) \times \left( 1 + 5^{\left( T_{27} - 866 \right) / 10.42} \right)$ | |
| Condenser | $Z_{\mathrm{cond.,PP}} = 248 \times A_{CD,PP} + 659 \times m_{35}$ | [62] |
| Generator section | $Z_{gen,GT} = 60 \times \dot{W}_{GT}^{\ 0.95}$ | [64] |
| | $Z_{gen,ST} = 60 \times \dot{W}_{ST}^{\ 0.95}$ | |
| Pump section | $Z_{\mathrm{HRSG,P}} = 378 \times \left( 1 + \left( \left( 1 - \eta_p \right) / \left( 1 - 0.83 \right) \right)^3 \times X_{30}^{\ 0.71} \right)$ | [63] |
| | $Z_{\mathrm{HRSG,MED,P}} = 378 \times \left( 1 + \left( \left( 1 - \eta_p \right) / \left( 1 - 0.83 \right) \right)^3 \times X_{32}^{\ 0.71} \right)$ | |
| | $Z_{\mathrm{cond,PP,P}} = 378 \times \left( 1 + \left( \left( 1 - \eta_p \right) / \left( 1 - 0.83 \right) \right)^3 \times X_{34}^{\ 0.71} \right)$ | |

| | | |
|---|---|---|
| HRSG | $$Z_{HRSG} = C_{\mathrm{HRSG},1} \times \left( \begin{array}{l} \left( C_{\mathrm{HRSG,P1}} \times C_{\mathrm{HRSG,ST1}} \times C_{\mathrm{HRSG,GT1}} \times \left( \dot{Q}_{HRSG,1} / LMTD_{HRSG,1} \right)^{0.8} \right) \\ + \left( C_{\mathrm{HRSG,P2}} \times C_{\mathrm{HRSG,ST2}} \times \left( \dot{Q}_{HRSG,2} / LMTD_{HRSG,2} \right)^{0.8} \right) \end{array} \right) + \left( C_{\mathrm{HRSG},2} \times \left( \left( C_{\mathrm{HRSG,P1}} \times m_{24} \right) + \left( C_{\mathrm{HRSG,P2}} \times m_{26} \right) \right) \right) + \left( C_{\mathrm{HRSG},3} \times m_{23}^{1.2} \right)$$ | [61,62] |

**Table 5.**
Input exergoeconomic analysis features [45–47].

| **Features** | **Nominal value** |
|---|---|
| Amortization duration *t*, years | 30 |
| Interest rate *i*, % | 5 |
| Cost index, $C_{index}$ | 1.2 |
| Electricity price $C_{ele}$, *$/kWh* | 0.06 |
| Annual availability, % | 90 |
| Steam heating cost, *$/kJ* | 1.466 |
| Chemical cost $C_{chemical}$, $\$/m^3$ | 0.025 |
| Maintenance cost | 2% of Z |
| Labor cost | $0.1\$/\dot{m}_D^3$ |

After the capital cost rate, a general cost balance equation is applied to each component of the system to calculate the stream outlet cost as given in Eq. 14. Similarly, the cost balance equations for all the components in the system are developed and presented in Table 6.

$$C_{out} = \sum C_{in} + \dot{Z} \tag{14}$$

A detailed discussion regarding the calculation of purchased equipment cost in terms of correlations, applicability ranges and other thermal design procedure for evaporators, preheaters, etc. have been presented in detail in previous studies by the authors [20,48].

**Table 6.**

Cost rates of the streams of Figure 2.

| Equipment | Correlations | Eq. # |
|---|---|---|
| Compressor | $C_{21} = C_{20} + C_{ele}\dot{W}_{comp} + \dot{Z}_{comp}$ | (15) |
| Combustion chamber | $C_{22} = C_{21} + C_f \times A + \dot{Z}_{comb}$ | (16) |
| Gas turbine section | $C_{23} = C_{22} - C_{36} + \dot{Z}_{GT}$ | (17) |
| | $C_{25} = C_{24} + \dot{Z}_{HPST} - C_{38}$ | (18) |
| Steam turbine section | $C_{27} = C_{26} + \dot{Z}_{MPST} - C_{39}$ | (19) |
| | $C_{28} = C_{27} - C_{14} + \dot{Z}_{LPST} - C_{40}$ | (20) |
| Condenser | $C_{29} = C_{28} + C_{34} - C_{35} + \dot{Z}_{Cond,PP}$ | (21) |
| Generator section | $C_{37} = C_{36} + \dot{Z}_{Gen,GT}$ | (22) |
| | $C_{41} = C_{40} + \dot{Z}_{Gen,ST}$ | (23) |
| HRSG | $C_{24} = C_{23} + C_{25} + C_{30} + C_{32} + \dot{Z}_{HRSG} - C_{26} - C_{31}$ | (24) |
| Pumps | $C_{34} = C_{33} + C_{ele}\dot{W}_{Cond,PP,P} - C_{35} + \dot{Z}_{Cond,PP,P}$ | (25) |
| | $C_{30} = C_{29} + C_{ele}\dot{W}_{HRSG,P} + \dot{Z}_{HRSG,P}$ | (26) |
| | $C_{32} = C_{19} + C_{ele}\dot{W}_{HRSG,MED,P} + \dot{Z}_{HRSG}$ | (27) |
| Electricity cost | $C_{ele,PP} = C_{37} + C_{41} + C_{35} + C_{31}$<br>$C_{ele}(\$/kJ) = \frac{C_{ele,PP}}{\dot{W}_{net}}$ | (28) |

It is worth mentioning that in all the equations with multi output flows, auxiliary equations are needed to solve the cost balance. These auxiliary equations can be developed using any of the following three methods [49]: equality method, extraction method, and by-product method. The first one (the equality method) is based on the concept of equal priority of both products and works by equating the exergy costs of both products e.g., work, and low-pressure steam in the case of a steam turbine. While the second one (i.e., the extraction method) works by considering the purpose of certain machines/equipment e.g., the purpose of a turbine is to produce shaft power, hence the stream cost must be calculated by giving priority to only the work output. Therefore, the auxiliary

equation will equate the exergy cost of high and low-pressure steam at the inlet and outlet of the turbine. While the by-product method considers the low-pressure steam as a by-product that will be produced even if the turbine is generating no power. Hence, it assigns a certain cost to the by-product stream, and the cost of produced work is determined from the exergy cost balance between work and inlet stream [50]. Based on the above discussion, the auxiliary equations for turbine are as follows:

$$\frac{C_{24}}{X_{24}} = \frac{C_{25}}{X_{25}} \tag{29}$$

$$\frac{C_{26}}{X_{26}} = \frac{C_{27}}{X_{27}} \tag{30}$$

$$\frac{C_{27}}{X_{27}} = \frac{C_{28}}{X_{28}} \tag{31}$$

Finally, the payback period representing the duration in which the investment made on the integration of MED is recovered by selling the freshwater is calculated as:

$$Payback\ period = \frac{Initial\ \ investment}{Net\ amount\ recovered} \tag{32}$$

Moreover, the break-even point at which all the investment is paid back is also determined for the project as a point where fixed cost and variable cost lines cut each other. After this point, the system operation generates profit.

## 4. Sensitivity analysis

It is an important tool to critically investigate the effect of input parameters on the system performance to highlight the most influential ones for future developments [51]. In this regard, the derivative-based sensitivity evaluation is among the most typical and effective techniques in which each input parameter is introduced as a sum of its nominal value and the perturbation [52]. Meanwhile, a more reliable and robust way of presenting the parametric sensitivity is the Normalized Sensitivity Analysis which uses the Normalized Sensitivity Coefficients (NSC) instead of simple partial derivatives. These NSCs allow a rationale comparison of parameters with significantly different magnitudes. This is because the NSCs are obtained by normalizing the perturbations in the response and input parameters by corresponding nominal values [53]. For instance, let the performance parameter be "*r"* and $r = r\,(x_1, x_2, x_3, \ldots x_j)$ then the perturbation $U_r$ in the performance parameter "*r*" due to perturbation about the nominal value of an independent process parameter is found by the following formula [54]:

$$U_r = \left[ \left( \frac{\partial r}{\partial x_1} U_{\mathrm{x},1} \right)^2 + \left( \frac{\partial r}{\partial x_2} U_{\mathrm{x},2} \right)^2 + \ldots\ldots\ldots + \left( \frac{\partial r}{\partial x_j} U_{\mathrm{x,j}} \right)^2 \right]^{1/2} \tag{33}$$

Where, $U_{x,j}$ terms in the equation show the perturbation about nominal values of process parameters, and $\partial r/\partial x$ terms are known as sensitivity coefficients. Then sensitivity of the output parameter upon selected input variables is normalized to the nominal value of *r*. The mathematical description of the process is as follows [52].

$$\frac{U_r}{\bar{r}} = \left[ \sum_{j=1}^{n} \left\{ \left( \frac{\partial r}{\partial x_j} \frac{\bar{x}_j}{\bar{r}} \right) \left( \frac{U_{x,j}}{\bar{x}_j} \right) \right\}^2 \right]^{1/2} \tag{34}$$

Here, $\bar{r}$ and $\bar{x}$ are the nominal values and the dimensionless terms $\left( \frac{\partial r}{\partial x_j} \frac{\bar{x}_j}{\bar{r}} \right)^2$ are known as the normalized sensitivity coefficients which are of interest for this study. The physical significance of finding these coefficients is to quantify the variation in a performance parameter due to certain disturbances in a process parameter [55].

Besides NSC, Relative Contribution (RC) is another important parameter to distinguish the dominant sensitivity contributors by combining the sensitivity coefficients with the actual perturbation. It is obtained as the square of the product of sensitivity coefficient and perturbation,

normalized by the square of the perturbation in the response parameter.

$$RC = \frac{\left(\frac{\partial r}{\partial x_j} U_{x,j}\right)^2}{U_r^2} \tag{35}$$

## 5. Results and discussion

### *5.1. Model validation*

The mathematical model for the CCGT power plant is first validated with the actual plant data reported in the literature by Shahzad et al. [39]. For this purpose, the system is operated on the same process parameters i.e., temperature and mass flow rates as adopted in the literature [39]. Thermal efficiency and Exergy efficiency are used as validation parameters as presented in Figure 3. A very close agreement is seen in both sets of values with a maximum discrepancy of ±1.71% which confirms the model validity. The small deviation is because of the difference in thermophysical properties which are calculated in the current study using EES, while in the literature these are calculated using standard steam tables corresponding to actual plant data.

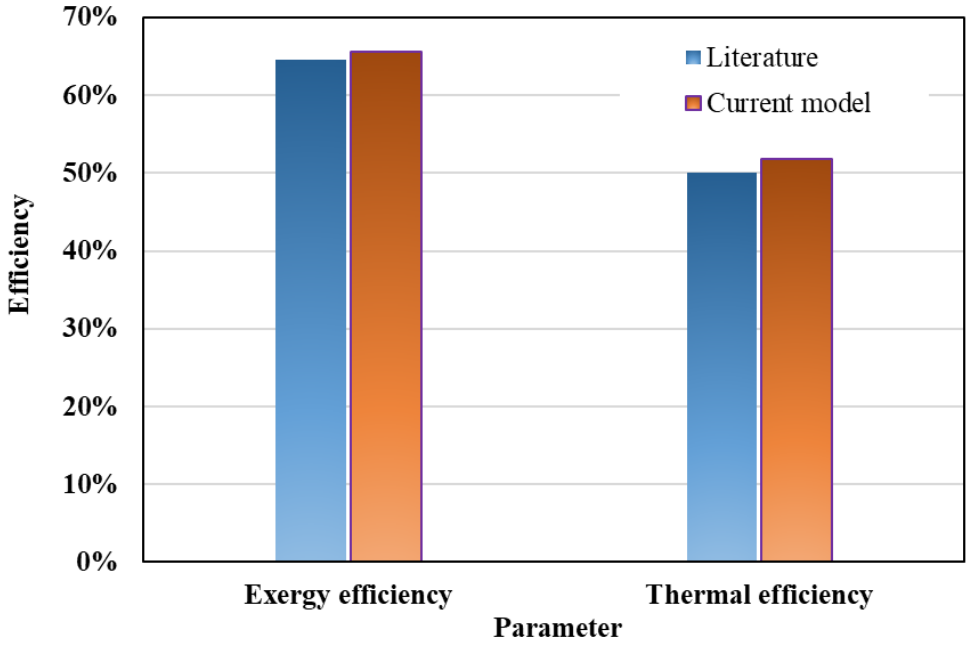


**Figure 3.** Numerical CCGT model validation with the literature [39].

### *5.2. Thermodynamic analysis*

The thermodynamic performance of the system is measured from energy and exergy viewpoints. For energy analysis, the thermal efficiency of gas turbine, steam turbine, and overall power plant are evaluated. Figure 4 shows the thermal efficiencies for gas turbine, steam turbine, and overall power plant as 51.72%, 32.66%, and 57.66%, respectively. The corresponding exergy efficiencies (refer to Figure 5) for these turbines are calculated as 65.66%, 51.81%, and 59.93%, respectively. Meanwhile, for a more detailed analysis, the exergy destruction in each component of the system is calculated using the general exergy balance equation. Figure 6 shows that the maximum exergy destruction occurred in the combustion chamber with 32% followed by compressor with 28%, a low-pressure turbine 21% (relatively high because of steam bleeding), condenser 7%, gas turbine 4%, medium pressure turbine 3%, high-pressure turbine 2%, and HRSG 2%. Meanwhile, it is important to emphasize that, only 1% of the total exergy destruction occurred in the desalination system. The overall exergy destruction in the system (CCGT+MED) is calculated as 540 MW.

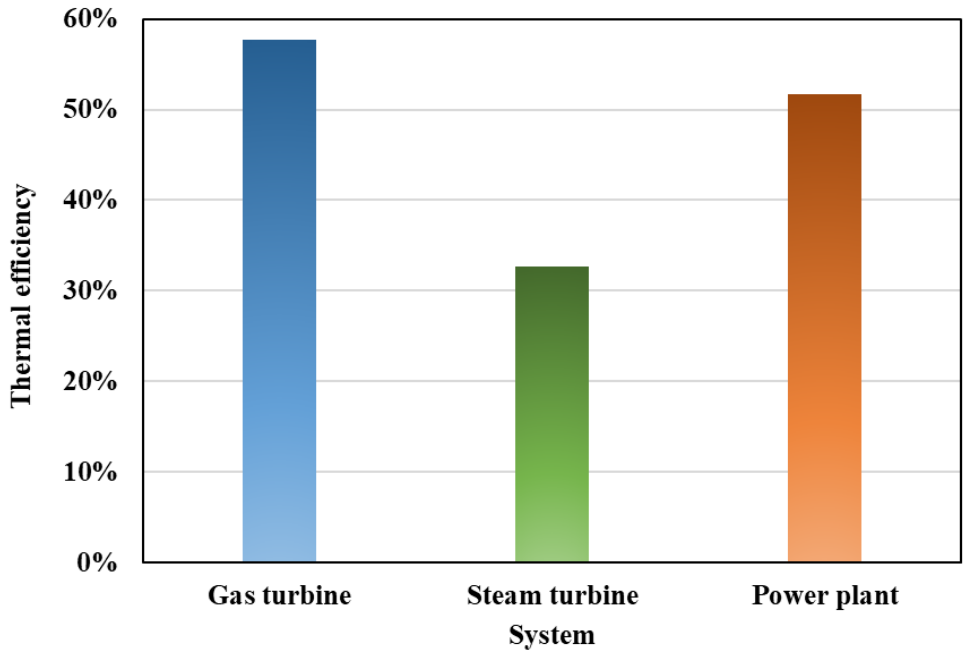


**Figure 4.** Thermal efficiencies of turbines and power plant.

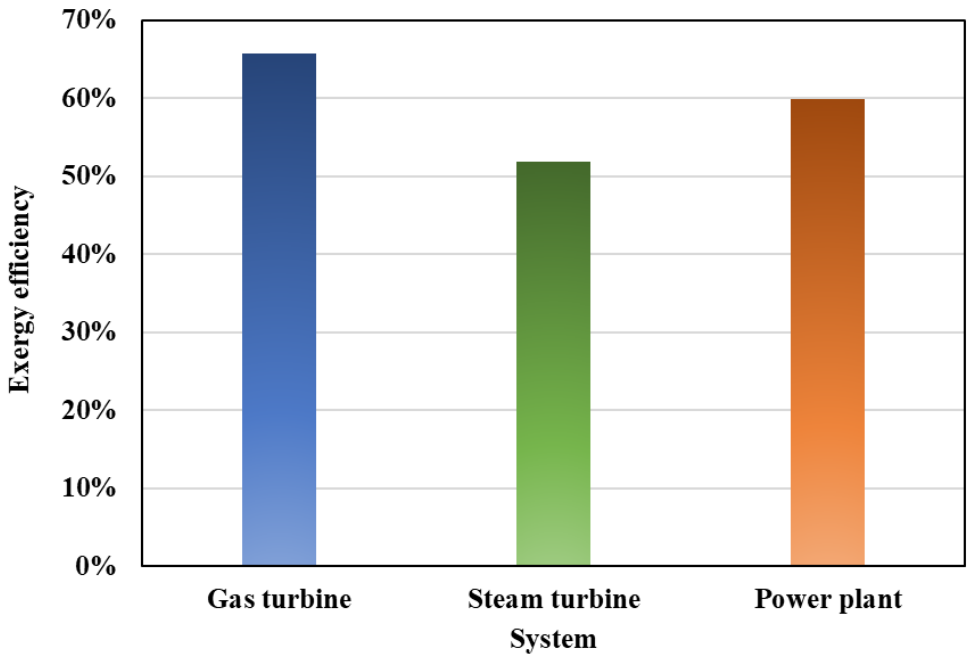


290
291 **Figure 5.** Second law efficiency of the power plant.

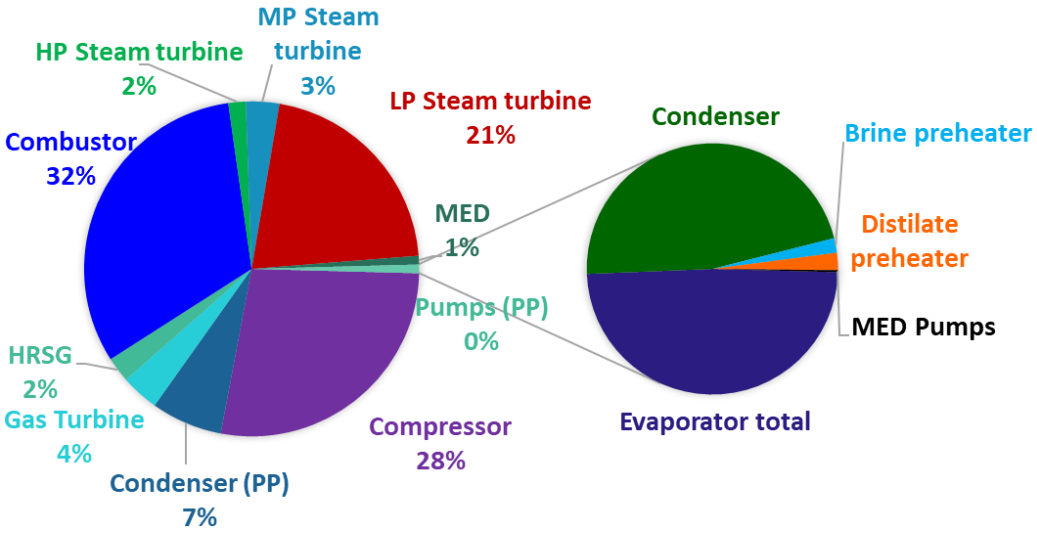


292
293 **Figure 6.** Equipment-based exergy destruction of CCGT+MED.

294

### *5.3. Exergoeconomic analysis*

Following the energy and exergy analyses, a detailed exergoeconomic investigation of the system is conducted to highlight the monetary contribution of each component to the final products. For this purpose, the stream cost ($/h) at all state points of the power plant and desalination system and presented in Table 7. The analysis showed that the major contributions in the stream cost are in the power plant sections are from the compressor, and turbine sections while in desalination systems from evaporator sections. Thereafter, a parametric analysis using the one-factor-at-a-time approach is performed to study the effect of the input parameter on the products cost. Figure 7 shows the effect of fuel cost on the electricity and freshwater production cost. It is observed that the unit cost of electricity increased from $0.033 to 0.089/kWhr and for distillate $1.2 to 2.41/$m^3$ for the fuel cost varying from 0.072 to 0.22 $/$m^3$. Similarly, the effects of fuel heating values on the electricity and freshwater production cost are presented in Figure 8. It is observed that an increase in the heating value of the fuel decreased the electricity as well as freshwater production cost due to a decrease in the specific fuel consumption. The electricity cost decreased from $0.0529 to 0.04863/kWhr and the freshwater cost decreased from $1.644 to 1.552/$m^3$ when heating value decreased from 45 to 50 MJ/kg (which can vary with regions [56]). Similarly, the variation in electricity and freshwater production cost against interest rate is presented in Figure 9 which shows a direct impact on both cases.

Meanwhile, the comparison of product cost for CCGT+MED system with standalone MED and standalone MED with energy recovery preheaters (MED+ER) is also presented in Figure 10. The analysis showed that, the lowest product cost is observed for the hybrid CCGT+MED systems followed by MED+ER and MED. In MED+ER, the hot brine and distillate streams are used to preheat the intake seawater. This preheating reduces the sensible heat load in the evaporators thus reducing the energy input as well as evaporator size. Therefore, because of being energy efficient, these systems perform better than MED systems in which the high temperature brine is discarded in the sea. However, the current analysis showed that the CCGT+MED system observed 24% less water production cost than the MED+ER system. Moreover, its is also observed that the product cost decreased as the number of evaporators increased in all the cases. Similarly, the product cost for MED+ER and CCGT+MED against different interest rates is compared in Figure 11 which shows the lower cost for hybrid system at all conditions. A more detailed investigation and optimization of standalone MED systems under different configurations and similar process

parameter ranges are presented in a recent study by authors [48].

**Table 7.**

Cost Flow of CCGT+MED with energy recovery section.

| State Points | Cost ($/h) | State Points | Cost ($/h) |
|---|---|---|---|
| **0.** Feed pump inlet | 4.6 | **1.** Feed pump outlet | 10 |
| **2.** Feed to distillate preheater | 3.6 | **3.** Feed to brine preheater | 7.2 |
| **4.** Feed to distillate Preheater | 19 | **5.** Feed from brine preheater | 53 |
| **6.** Feed of first evaporator | 72 | **7.** Last effect brine to preheater | 44 |
| **8.** Condensate to preheater | 17 | **9.** Brine from brine preheater | 2.9 |
| **10.** Brine pump outlet | 3.2 | **11**. Distillate from preheater | 3.8 |
| **12.** Distillate from distillate pump | 6.5 | **13.** Last effect vapors to condenser | 160 |
| **14.** Bleed steam from LP turbine | 97 | **15.** Cooling water to condenser | 6.8 |
| **16.** Cooling water out | 196 | **17.** Condensate from condenser | 2.1 |
| **18.** Total distillate | 5.86 | **19.** Steam condensate | 4.9 |
| **20.** Compressor air inlet | 0 | **21.** Compressed air outlet | 11581 |
| **22.** Combustor chamber outlet | 21412 | **23.** Gas turbine outlet / HRSG inlet | 8755 |
| **24.** HP turbine inlet | 8305 | **25.** HP turbine steam out | 6271 |
| **26.** MP turbine inlet | 7592 | **27.** LP turbine inlet | 5205 |
| **28.** LP turbine outlet condenser | 931 | **29.** Condenser outlet | 675 |
| **30.** Inlet cooling water to HRSG | 675 | **31.** HRSG outlet | 181 |
| **32.** Steam condensate to HRSG | 5.2 | **33.** Cooling water pump inlet | 4.6 |
| **34.** Cooling water to condenser | 4.7 | **35.** Cooling water outlet | 262 |
| **36.** Gas turbine outlet | 12657 | **37.** Gas turbine generator outlet | 12844 |
| **38.** HP turbine out | 2133 | **39.** MP turbine out | 2510 |
| **40.** LP turbine out | 4262 | **41.** LP turbine generator out | 4330 |

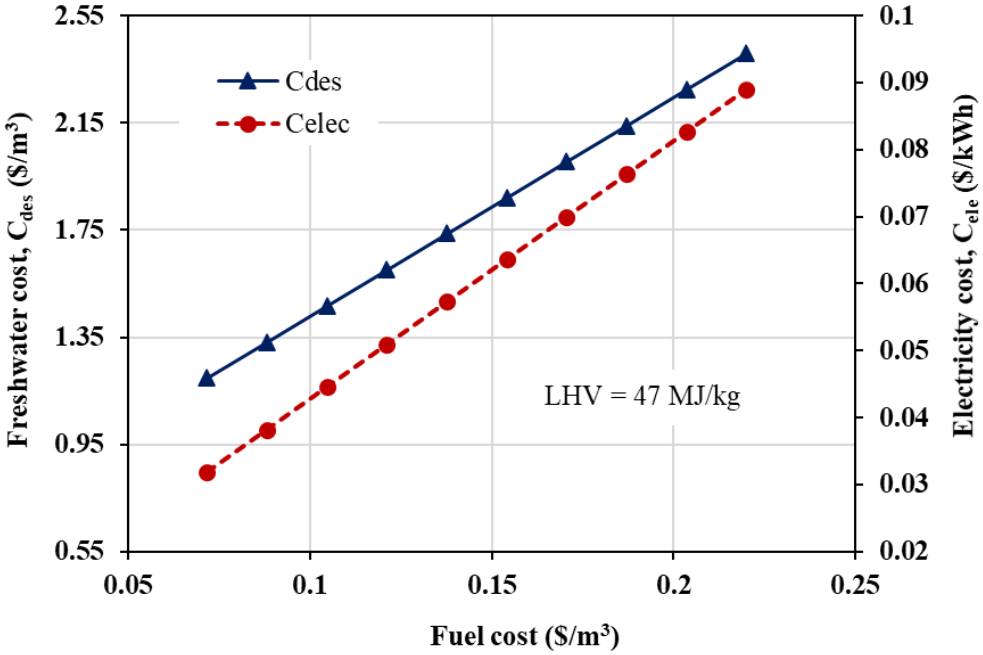


330

331 **Figure 7.** Effect of fuel cost on electricity and freshwater production costs.

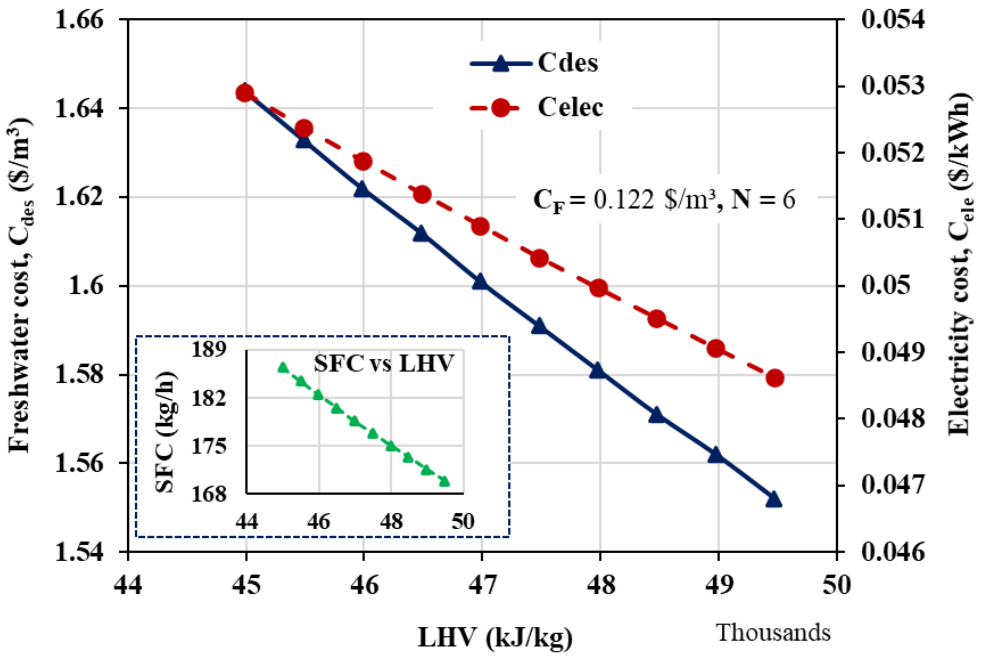


332

333 **Figure 8.** Effect of fuel heating value on specific fuel consumption, electricity, and freshwater

334 production costs.

335

336

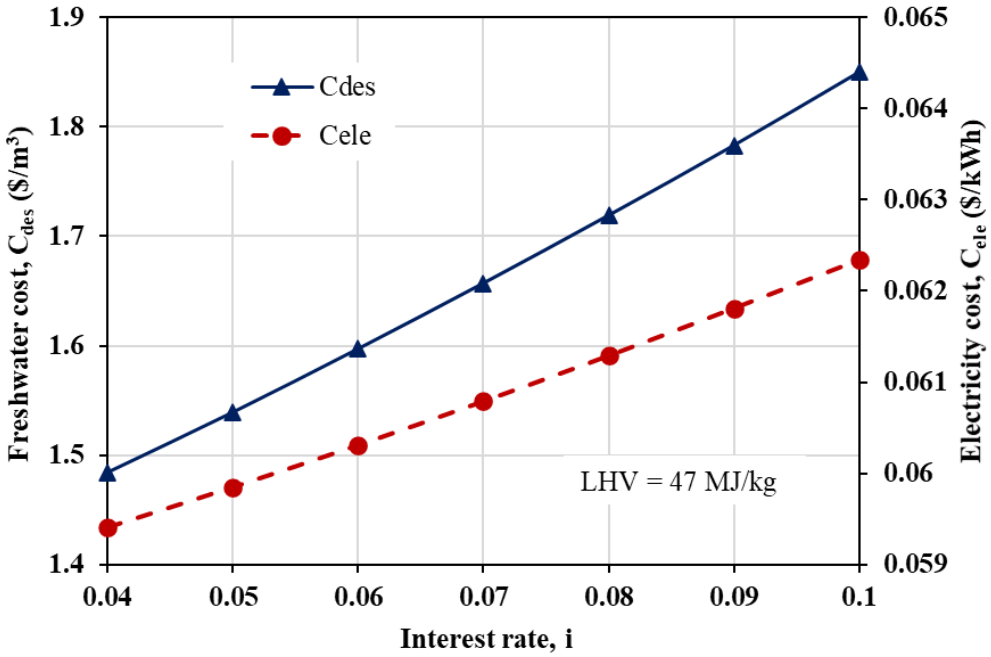


337

338 **Figure 9.** Effect of interest rate on the electricity and freshwater production costs.

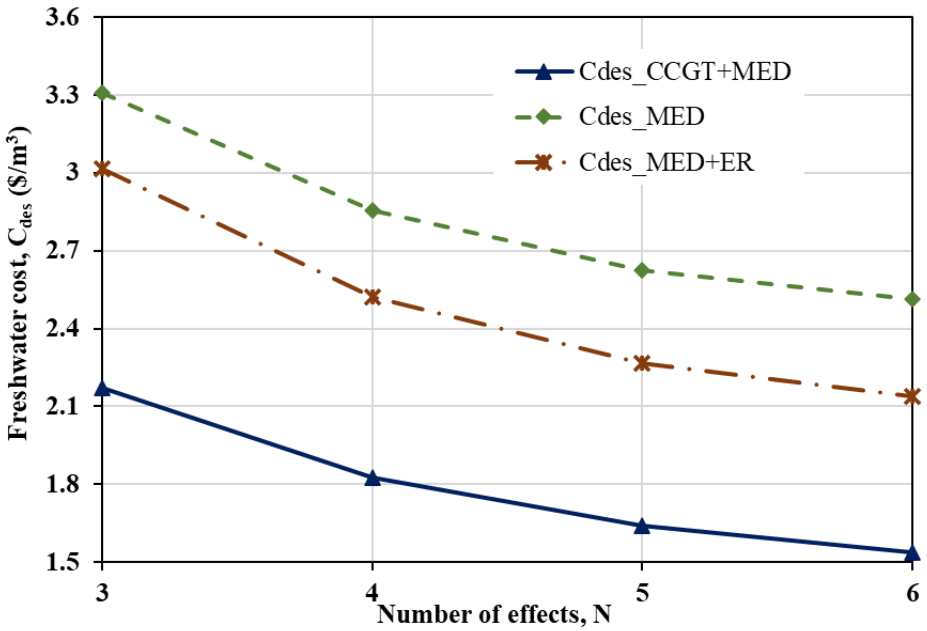


339

340 **Figure 10.** Freshwater production cost comparison between MED, MED+ER and
341 CCGT+MED at different number of evaporators.
342

343

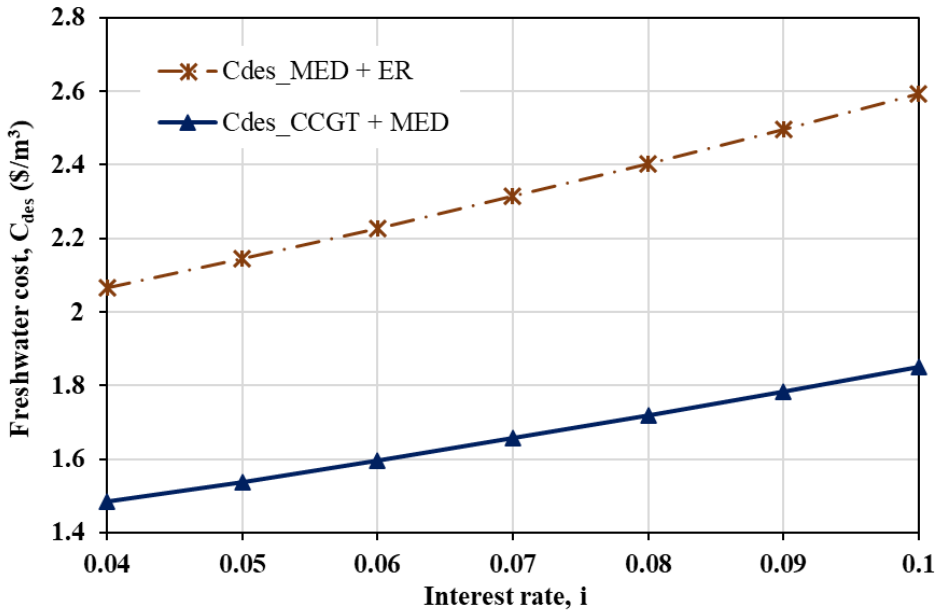


**Figure 11.** Effect of interest rate on the electricity and freshwater production costs.

Figure 12 shows a variation in the capital investment/ fixed cost of the desalination system with the desalination capacity based on the correlations presented in Table 3 and Table 4. The fixed cost of the MED system increased from 6 to 16 M$ when the desalination capacity enhanced from 50 to 120 kg/s. This massive increase in the cost is because of an increase in the heat transfer area which controls the desalination capacity as well as the investment cost. Meanwhile, it is also important to note that an increase in desalination capacity, decreased the freshwater production cost as shown in Figure 13. The freshwater cost decreased from1.662 to 1.611 $/m$^3$ by increasing plant capacity from 50 to 120 kg/s. This decrease in unit freshwater cost is because of low operational cost which dominated the effect of capital cost at higher capacities. It shows a higher influence of operational cost on the freshwater production cost than the initial investment. Finally, Figure 14 shows the installation cost of the desalination plant with an existing power plant. A total investment of $6897000 is made to install a MED system in year 1. From the next year, the revenue generation by selling the fresh water at the cost rate is counted on an annual basis. This takes 3.99 years to break even all the invested cost and the plant life considered in the analysis of the system is 30 years. This shows that excluding a small period of 3.99 years, the system will generate profit for the remaining life of 26.01 years without any major capital investment.

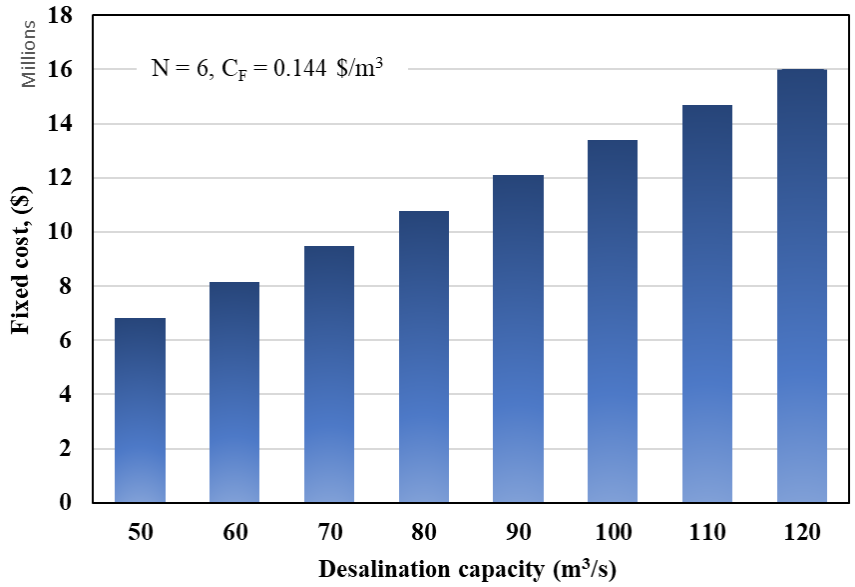


362

363 **Figure 12.** Desalination capacity versus capital/fixed cost.

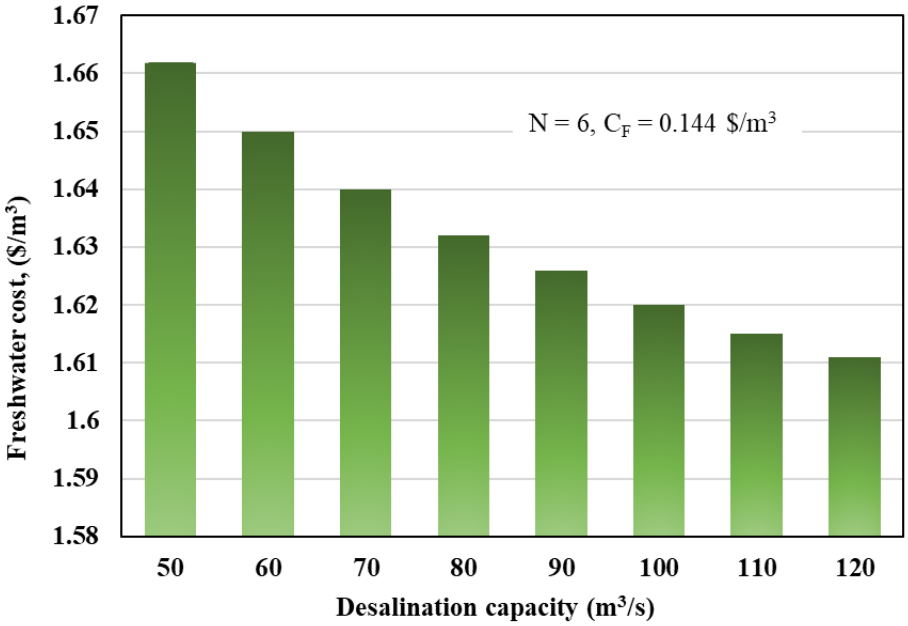


364

365 **Figure 13.** Desalination capacity versus freshwater production cost.

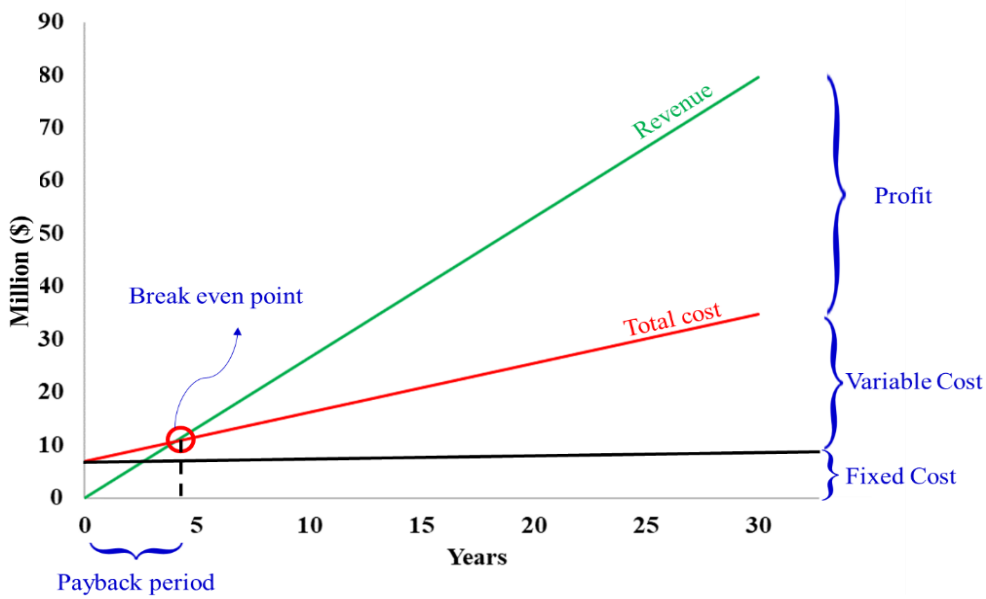


366

367 **Figure 14.** Annual revenue generation and breakeven point.

368

### *5.4. Sensitivity analysis*

The outcomes of sensitivity analysis are presented in terms of Normalized Sensitivity Coefficients (NSCs) and Relative Contribution (RC). The output parameters are electricity cost ($C_{ele}$), and desalinated water cost ($C_{des}$). While the input parameters include fuel cost (C_fuel), cost index factor (C_ind), interest rate (i), gas turbine efficiency (η_GT), high-pressure steam turbine efficiency (η_HPST), medium pressure steam turbine efficiency (η_MPST), low-pressure steam turbine efficiency (η_LPST), and lower heating value of the fuel (LHV). For this analysis, the values of these input parameters are modeled as a sum of their nominal value and a perturbation of ±1% of the nominal (refer to Table 8**),** and the results are presented for parameters with NSC≥ 0.001.

**Table 8.**
Nominal and perturbation values of parameters of sensitivity analysis.

| **Input parameter** | **Nominal value** | **Perturbation** |
|---|---|---|
| Fuel cost, C_fuel, \$/ 1000ft$^3$ | 4.13 | ±0.0413 |
| Cost index factor, C_ind | 1.2 | ±0.012 |
| Interest rate, i | 0.05 | ±0.0005 |
| Gas turbine efficiency, η_GT | 0.83 | ±0.0083 |
| High-pressure steam turbine efficiency, η_HPST | 0.77 | ±0.0077 |
| Medium pressure steam turbine efficiency, η_MPST | 0.73 | ±0.0073 |
| Low-pressure steam turbine efficiency, η_LPST | 0.48 | ±0.0048 |
| The lower heating value of the fuel, LHV, kJ/kg | 47230 | ±472 |

Figure 15 shows the sensitivity of $C_{ele}$ and it is observed that $C_{elec}$ is the most sensitive to η_GT with NSC = 1.71, followed by C_fuel with NSC = 0.86 and LHV with NSC = 0.80. The other input parameters have relatively low impact on Cele in the following order η_MPST > η_HPST η_LPST > C_ind > i with NSCs varying between 0.03 to 0.0014. Similarly, the relative contribution for these parameters is as follows $RC_{\eta\_GT}$ = 49.4%, $RC_{C\_fuel}$ = 24.8%, $RC_{LHV}$ = 23.1%, and for other parameters is relatively low as follows $RC_{\eta\_MPST}$ = 0.95%, $RC_{\eta\_HPST}$ = 0.87%, $RC_{\eta\_LPST}$ = 0.49% $RC_{C\_ind}$ = 0.12%, and $RC_i$ = 0.04%. Likewise, Figure 16 shows that $C_{des}$ is the most sensitive to η_GT with NSC = 0.76, followed by C_fuel with NSC = 0.42 and LHV with NSC = 0.40. However,

in $C_{des}$ case, the influence of other parameters is different than the $C_{ele}$ case and follows the following order C_ind > i > η_MPST > η_HPST > η_LPST with NSCs 0.072, 0.023, 0.0046, 0.0042, and 0.0023, respectively. While the corresponding relative contribution for these parameters is as follows $RC_{\eta\_GT}$ = 45.1%, $RC_{C\_fuel}$ = 24.6%, $RC_{LHV}$ = 23.8%, $RC_{C\_ind}$ = 4.27%, $RC_{i}$ = 1.38%, $RC_{\eta\_MPST}$ = 0.27%, $RC_{\eta\_HPST}$ = 0.25%, and $RC_{\eta\_LPST}$ = 0.14%.

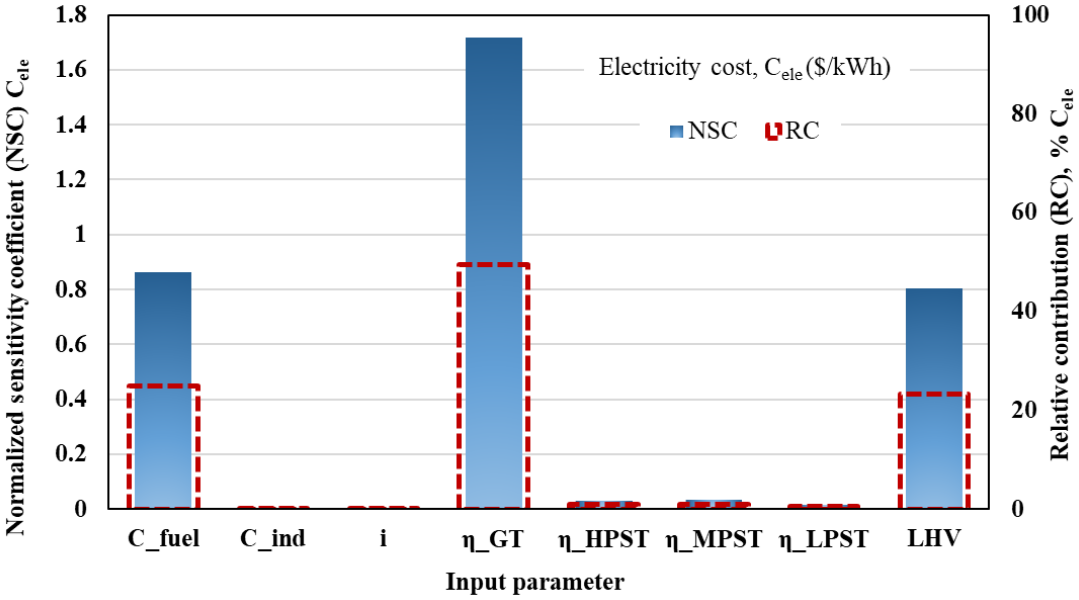


**Figure 15.** The sensitivity of electricity cost over fuel cost and LHV.

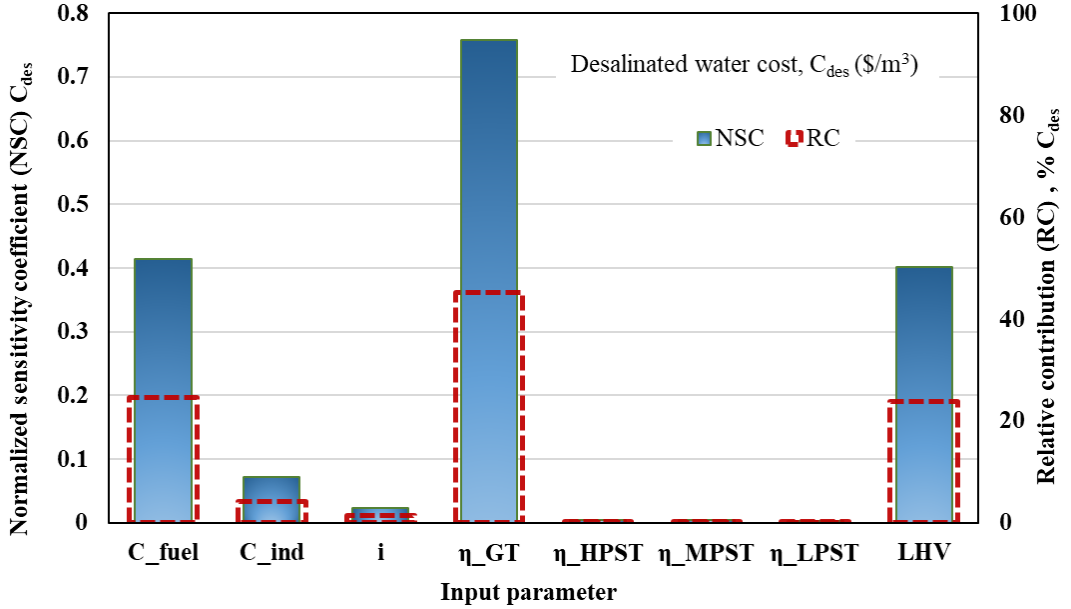


**Figure 16.** The sensitivity of distillate cost over fuel cost and LHV.

## 6. Conclusion

The exergoeconomic and normalized sensitivity analyses-based investigation of a hybrid combined cycle gas turbine and multi-effect desalination systems (CCGT+MED) is conducted. The energy consumption, exergy destruction, thermal and exergy efficiencies, stream costs, product costs, and the sensitivity of different input parameters on the products are assessed. Under the considered operating conditions, the following major outcomes are obtained.

- The cogeneration system reduced the electricity cost by 16.8% and freshwater production cost by 24.5% compared to the standalone MED system.
- An increase in fuel cost from \$0.072/$m^3$ to \$0.22 /$m^3$, increased the electricity production cost from \$0.033/kWhr to \$0.089/kWhr, and the corresponding freshwater cost from \$1.2/$m^3$ to \$2.41/$m^3$.
- An increase in LHV of the fuel from 45 to 50 MJ/kg, decreased the electricity production cost from \$0.0529/kWhr to \$0.04863/kWhr and distillate cost from \$1.644/$m^3$ to \$1.552/$m^3$ because of a decrease in the specific fuel consumption.
- An increase in the freshwater production capacity from 50 to 120kg/s, increased the capital investment of the MED section from 6.8 M\$ to 16 M\$ because of higher heat transfer area requirements. However, it reduced the freshwater production cost from \$1.662/$m^3$ to \$1.611/$m^3$ because of the dominancy of operation cost over the capital cost at higher productivities.
- Sensitivity analysis showed that the electricity production cost $C_{ele}$ turned out to be the most sensitive to η_GT, followed by C_fuel and LHV with NSCs of 1.71, 0.86, and 0.80, respectively. While other parameters like steam turbine efficiencies, cost index factor, and interest rate showed very low impact on $C_{ele}$ with NSCs varying between 0.0014 to 0.03. Similar trend was observed for the relative contribution of parameters as well.
- The desalinated/freshwater production cost $C_{des}$ showed the most sensitivity to η_GT with NSC = 0.76, followed by C_fuel with NSC = 0.42 and LHV with NSC = 0.40. while the other parameters showed the following order C_ind > i > η_MPST > η_HPST > η_LPST with NSCs 0.072, 0.023, 0.0046, 0.0042, and 0.0023, respectively. Similar trend for relative contribution was also observed.

**Acknowledgment**

The authors acknowledge the support provided by Northumbria University, UK under reference # RDF20/EE/MCE/SHAHZAD and MCE QR funds 2020/21.

**Nomenclature**

| | |
|---|---|
| B | brine |
| $\dot{C}$ | the rate of monetary cost ($/s) |
| C | stream $/s |
| $C_p$ | specific heat, kJ/kg |
| $C_{ind}$ | cost index factor |
| h | enthalpy kJ/kg |
| $i$ | interest rate |
| $\dot{m}$ | mass flow rate, kg/s |
| Nu | Nusselt number |
| P | pressure, kPa |
| Pr | Prandtl number |
| $\dot{Q}$ | heat transfer rate, kW |
| $r$ | output/dependent variable for sensitivity analysis |
| Re | Reynolds number |
| $S$ | salinity, g/kg |
| s | entropy, kJ/kg K |
| $T$ | temperature ($^o$C) |
| $\dot{V}$ | volume flow rate ($m^3$/s) |
| $\dot{W}$ | work, kW |
| $X$ | exergy, kW |
| $x$ | Input/independent variables for sensitivity analysis |
| $Z$ | fixed cost ($) |
| $\dot{Z}$ | rate of fixed cost ($/s) |
| *Greek letters* | |
| $\Delta$ | change in quantity |

| | |
|---|---|
| $\rho$ | density |
| $\Upsilon$ | feed mass flow per unit length of each side of the tube |
| $\eta$ | efficiency |
| *Subscripts* | |
| II | second law/exergy |
| B | brine |
| CD | condenser |
| Comp | compressor |
| D | distillate |
| EV | evaporator |
| F | feed |
| N | number of effects |
| P | product |
| 0 | dead state |
| *Superscripts* | |
| $t$ | plant life in years |
| *Abbreviations* | |
| AR | absorption refrigeration |
| B-PH | brine preheater |
| $Bm^3$ | billion cubic meters |
| BP | brine pump |
| BPE | boiling point elevation |
| CCGT | combined-cycle gas turbine |
| CD | condenser |
| CRF | capital recovery factor |
| CWP | cooling water pump |
| D-PH | distillate preheater |
| DP | distillate pump |
| EC | evaporative cooler |
| EES | engineering equation solver |
| FF-MED | forward feed multi-effect desalination |

| | |
|---|---|
| FP | feed pump |
| GT | gas turbine |
| HDH | humidification dehumidification |
| HPST | high-pressure steam turbine |
| HRSG | heat recovery steam generation |
| LHV | lower heating value, kJ/kg |
| LNG | liquified natural gas |
| LPST | low-pressure steam turbine |
| MED | multi-effect desalination |
| $Mm^3$ | million cubic meters |
| MPST | medium pressure steam turbine |
| MSF | multi-stage flash |
| MVC | mechanical vapor compression |
| NSA | normalized sensitivity analysis |
| NSC | normalized sensitivity coefficient |
| PP | power plant |
| RC | relative contribution |
| RO | reverse osmosis |
| SEC | specific energy consumption |
| TVC | thermal vapor compression |

433

434

## References


[1] Altmann T, Robert J, Bouma A, Swaminathan J, Lienhard JH. Primary energy and exergy of desalination technologies in a power-water cogeneration scheme. Appl Energy 2019;252:113319. https://doi.org/10.1016/j.apenergy.2019.113319.

[2] Ding H, Li J, Heydarian D. Energy, exergy, exergoeconomic, and environmental analysis of a new biomass-driven cogeneration system. Sustain Energy Technol Assessments 2021;45:101044. https://doi.org/10.1016/j.seta.2021.101044.

[3] Shahzad MW, Burhan M, Ang L, Choon Ng K. Energy-water-environment nexus underpinning future desalination sustainability. Desalination 2017;413:52–64. https://doi.org/10.1016/j.desal.2017.03.009.

[4] Yaqoob H, Heng Y, Din ZU, Sabah NU, Jamil MA, Mujtaba MA, et al. The potential of sustainable biogas production from biomass waste for power generation in Pakistan. J Clean Prod 2021;307:127250. https://doi.org/10.1016/j.jclepro.2021.127250.

[5] Chen Q, Burhan M, Shahzad MW, Ybyraiymkul D, Akhtar FH, Li Y, et al. A zero liquid discharge system integrating multi-effect distillation and evaporative crystallization for desalination brine treatment. Desalination 2021;502:114928. https://doi.org/10.1016/j.desal.2020.114928.

[6] Khanmohammadi S, Khanjani S. Experimental study to improve the performance of solar still desalination by hydrophobic condensation surface using cold plasma technology. Sustain Energy Technol Assessments 2021;45:101129. https://doi.org/10.1016/j.seta.2021.101129.

[7] Esmaeilion F. Hybrid renewable energy systems for desalination. Appl Water Sci 2020;10:1–47. https://doi.org/10.1007/s13201-020-1168-5.

[8] Jones E, Qadir M, van Vliet MTH, Smakhtin V, Kang S mu. The state of desalination and brine production: A global outlook. Sci Total Environ 2019;657:1343–56. https://doi.org/10.1016/j.scitotenv.2018.12.076.

[9] Shahzad MW, Burhan M, Ybyraiymkul D, Ng KC. Desalination processes ' efficiency and future roadmap. Entropy 2019;21:84. https://doi.org/10.3390/e21010084.

[10] Askalany AA, Ali ES. A new approach integration of ejector within adsorption desalination cycle reaching COP higher than one. Sustain Energy Technol Assessments 2020;41:100766. https://doi.org/10.1016/j.seta.2020.100766.

[11] Gevez Y, Dincer I. Development of an integrated system with desalination and heat storage options. Sustain Energy Technol Assessments 2021;45:101177. https://doi.org/10.1016/j.seta.2021.101177.
[12] Son HS, Shahzad MW, Ghaffour N, Ng KC. Pilot studies on synergetic impacts of energy utilization in hybrid desalination system: Multi-effect distillation and adsorption cycle (MED-AD). Desalination 2020;477:114266. https://doi.org/10.1016/j.desal.2019.114266.
[13] Wakil Shahzad M, Burhan M, Soo Son H, Jin Oh S, Choon Ng K. Desalination processes evaluation at common platform: A universal performance ratio (UPR) method. Appl Therm Eng 2018;134:62–7. https://doi.org/10.1016/j.applthermaleng.2018.01.098.
[14] Jamil MA, Goraya TS, Ng KC, Zubair SM, Bin B, Shahzad MW. Optimizing the energy recovery section in thermal desalination systems for improved thermodynamic , economic , and environmental performance. Int Commun Heat Mass Transf 2021;124:105244. https://doi.org/10.1016/j.icheatmasstransfer.2021.105244.
[15] Jamil MA, Din ZU, Goraya TS, Yaqoob H, Zubair SM. Thermal-hydraulic characteristics of gasketed plate heat exchangers as a preheater for thermal desalination systems. Energy Convers Manag 2020;205:112425.
[16] Alrowais R, Qian C, Burhan M, Ybyraiymkul D, Wakil M, Choon K. A greener seawater desalination method by direct-contact spray evaporation and condensation ( DCSEC ): Experiments. Appl Therm Eng 2020;179:115629. https://doi.org/10.1016/j.applthermaleng.2020.115629.
[17] Qian C, Alrowais R, Burhan M, Ybyraiymkul D. A self-sustainable solar desalination system using direct spray technology. Energy 2020;205:118037. https://doi.org/10.1016/j.energy.2020.118037.
[18] Jabari F, Nazari-heris M, Mohammadi-ivatloo B, Asadi S, Abapour M. A solar dish Stirling engine combined humidification-dehumidification desalination cycle for cleaner production of cool, pure water, and power in hot and humid regions. Sustain Energy Technol Assessments 2020;37:100642. https://doi.org/10.1016/j.seta.2020.100642.
[19] Jamil MA, Yaqoob H, Farooq MU, Teoh YH, Xu B Bin, Mahkamov K, et al. Experimental Investigations of a Solar Water Treatment System for Remote Desert Areas of Pakistan. Water 2021;13:1070. https://doi.org/10.3390/w13081070.
[20] Jamil MA, Shahzad MW, Zubair SM. A comprehensive framework for thermoeconomic

analysis of desalination systems. Energy Convers Manag 2020;222:113188.
[21] Jamil MA, Qureshi BA, Zubair SM. Exergo-economic analysis of a seawater reverse osmosis desalination plant with various retrofit options. Desalination 2016;401:88–98.
[22] Lienhard JH, Mistry KH, Sharqawy MH, Thiel GP. Thermodynamics, Exergy, and Energy Efficiency in Desalination Systems. 2017. https://doi.org/10.1016/B978-0-12-809791-5.00004-3.
[23] Ng KC, Burhan M, Chen Q, Ybyraiykul D, Akhtar FH, Kumja M, et al. A thermodynamic platform for evaluating the energy efficiency of combined power generation and desalination plants. Npj Clean Water 2021;4:1–10. https://doi.org/10.1038/s41545-021-00114-5.
[24] Jamil MA, Zubair SM. On thermoeconomic analysis of a single-effect mechanical vapor compression desalination system. Desalination 2017;420:292–307.
[25] Abdulrahim AH, Chung JN. Comparative thermodynamic performance study for the design of power and desalting cogeneration technologies in Kuwait. Energy Convers Manag 2019;185:654–65. https://doi.org/10.1016/j.enconman.2019.02.027.
[26] Almutairi A, Pilidis P, Al-Mutawa N, Al-Weshahi M. Energetic and exergetic analysis of cogeneration power combined cycle and ME-TVC-MED water desalination plant: Part-1 operation and performance. Appl Therm Eng 2016;103:77–91. https://doi.org/10.1016/j.applthermaleng.2016.02.121.
[27] Salehi S, Mahmoudi SMS, Yari M, Rosen MA. Multi-objective optimization of two double-flash geothermal power plants integrated with absorption heat transformation and water desalination. J Clean Prod 2018;195:796–809. https://doi.org/10.1016/j.jclepro.2018.05.234.
[28] Moradi M, Ghorbani B, Shirmohammadi R, Mehrpooya M, Hamedi MH. Developing of an integrated hybrid power generation system combined with a multi-effect desalination unit. Sustain Energy Technol Assessments 2019;32:71–82. https://doi.org/10.1016/j.seta.2019.02.002.
[29] Ghorbani B, Shirmohammadi R, Mehrpooya M. Development of an innovative cogeneration system for fresh water and power production by renewable energy using thermal energy storage system. Sustain Energy Technol Assessments 2020;37:100572. https://doi.org/10.1016/j.seta.2019.100572.
[30] Mohammadi K, Khaledi MSE, Saghafifar M, Powell K. Hybrid systems based on gas turbine combined cycle for trigeneration of power, cooling, and freshwater: A comparative techno-

economic assessment. Sustain Energy Technol Assessments 2020;37:100632. https://doi.org/10.1016/j.seta.2020.100632.

[31] Lee SH, Park K. Conceptual design and economic analysis of a novel cogeneration desalination process using LNG based on clathrate hydrate. Desalination 2021;498:114703. https://doi.org/10.1016/j.desal.2020.114703.

[32] Abdulrahim AH, Chung JN. Performance improvement of cogeneration plants in hot arid regions via sustainable turbine inlet air cooling technologies: An energy-water nexus comparative case study. Int J Energy Res 2021:1–29. https://doi.org/10.1002/er.6561.

[33] Sorgulu F, Dincer I. Development and assessment of a biomass-based cogeneration system with desalination. Appl Therm Eng 2021;185:116432. https://doi.org/10.1016/j.applthermaleng.2020.116432.

[34] Ding P, Liu X, Qi H, Shen H, Liu X, Farkoush SG. Multi-objective optimization of a new cogeneration system driven by gas turbine cycle for power and freshwater production. J Clean Prod 2021;288:125639. https://doi.org/10.1016/j.jclepro.2020.125639.

[35] Delpisheh M, Abdollahi Haghghi M, Mehrpooya M, Chitsaz A, Athari H. Design and financial parametric assessment and optimization of a novel solar-driven freshwater and hydrogen cogeneration system with thermal energy storage. Sustain Energy Technol Assessments 2021;45:101096. https://doi.org/10.1016/j.seta.2021.101096.

[36] Schmidt JM, Gude VG. Nuclear cogeneration for cleaner desalination and power generation – A feasibility study. Clean Eng Technol 2021;2:100044. https://doi.org/10.1016/j.clet.2021.100044.

[37] Tajik Mansouri M, Amidpour M, Ponce-Ortega JM. Optimization of the integrated power and desalination plant with algal cultivation system compromising the energy-water-environment nexus. Sustain Energy Technol Assessments 2020;42:100879. https://doi.org/10.1016/j.seta.2020.100879.

[38] Mohammadi K, McGowan JG. Thermodynamic analysis of hybrid cycles based on a regenerative steam Rankine cycle for cogeneration and trigeneration. Energy Convers Manag 2018;158:460–75. https://doi.org/10.1016/j.enconman.2017.12.080.

[39] Shahzad MW, Burhan M, Ng KC. A standard primary energy approach for comparing desalination processes. Npj Clean Water 2019:1–7. https://doi.org/10.1038/s41545-018-0028-4.

559 [40] Nayar KG, Sharqawy MH, Banchik LD, Lienhard V JH. Thermophysical properties of
560 seawater: A review and new correlations that include pressure dependence. Desalination
561 2016;390:1–24.
562 [41] Karakurt AS, Güneş Ü. Performance analysis of a steam turbine power plant at part load
563 conditions. J Therm Eng 2017;3:1121–8. https://doi.org/10.18186/thermal.298611.
564 [42] Ibrahim TK, Rahman MM. Effects of Isentropic Efficiency and Enhancing Strategies on Gas
565 Turbine Performance. J Mech Eng Sci 2013;4:383–96.
566 https://doi.org/10.15282/jmes.4.2013.3.0036.
567 [43] Jamil MA, Elmutasim SM, Zubair SM. Exergo-economic analysis of a hybrid humidification
568 dehumidification reverse osmosis (HDH-RO) system operating under different retrofits.
569 Energy Convers Manag 2018;158:286–97.
570 [44] Jamil MA, Zubair SM. Design and analysis of a forward feed multi-effect mechanical vapor
571 compression desalination system: An exergo-economic approach. Energy 2017;140:1107–
572 20.
573 [45] Elsayed ML, Mesalhy O, Mohammed RH, Chow LC. Transient performance of MED
574 processes with different feed confi gurations 2018;438:37–53.
575 https://doi.org/10.1016/j.desal.2018.03.016.
576 [46] Elsayed ML, Mesalhy O, Mohammed RH, Chow LC. Exergy and thermo-economic analysis
577 for MED-TVC desalination systems. Desalination 2018;447:29–42.
578 [47] Elsayed ML, Mesalhy O, Mohammed RH, Chow LC. Transient and thermo-economic
579 analysis of MED-MVC desalination system. Energy 2019;167:283–96.
580 [48] Abid A, Jamil MA, Sabah N us, Farooq MU, Yaqoob H, Khan LA, et al. Exergoeconomic
581 optimization of a forward feed multi-effect desalination system with and without energy
582 recovery. Desalination 2020;499:114808. https://doi.org/10.1016/j.desal.2020.114808.
583 [49] Abusoglu A, Kanoglu M. Exergoeconomic analysis and optimization of combined heat and
584 power production: A review. Renew Sustain Energy Rev 2009;13:2295–308.
585 https://doi.org/10.1016/j.rser.2009.05.004.
586 [50] El-Sayed YM, Gaggioli RA. A critical review of second law costing methods-I: Background
587 and algebraic procedures. J Energy Resour Technol Trans ASME 1989;111:1–7.
588 https://doi.org/10.1115/1.3231396.
589 [51] Ahmad M, Bin B, Dala L, Sultan M, Jie L, Wakil M. Experimental and normalized sensitivity

based numerical analyses of a novel humidifier-assisted highly efficient indirect evaporative cooler. Int Commun Heat Mass Transf 2021;125:105327. https://doi.org/10.1016/j.icheatmasstransfer.2021.105327.

[52] Jamil MA, Goraya TS, Shahzad MW, Zubair SM. Exergoeconomic optimization of a shell-and-tube heat exchanger. Energy Convers Manag 2020;226:113462.

[53] Qureshi BA, Qasem NAA, Zubair SM. Normalized sensitivity analysis of electrodialysis desalination plants for mitigating hypersalinity. Sep Purif Technol 2021;257:117858. https://doi.org/10.1016/j.seppur.2020.117858.

[54] Sarıdemir S, Ağbulut Ü. Combustion, performance, vibration and noise characteristics of cottonseed methyl ester–diesel blends fuelled engine. Biofuels 2019;0:1–10. https://doi.org/10.1080/17597269.2019.1667658.

[55] Qureshi BA, Zubair SM. A comprehensive design and rating study of evaporative coolers and condensers. Part II. Sensitivity analysis. Int J Refrig 2006;29:659–68.

[56] Farzaneh-Gord M, Rahbari HR, Nikofard H. The effect of important parameters on the natural gas vehicles driving range. Polish J Chem Technol 2012;14:61–8. https://doi.org/10.2478/v10026-012-0104-3.

[57] El-Sayed YM. Designing desalination systems for higher productivity. Desalination 2001;134:129–58.

[58] El-Mudir W, El-Bousiffi M, Al-Hengari S. Performance evaluation of a small size TVC desalination plant. Desalination 2004;165:269–79.

[59] Ettouney HM, El-Dessouky HT. Fundamentals of salt water Desalination. 2002.

[60] Abdelkader BA, Jamil MA, Zubair SM. Thermal-Hydraulic Characteristics of Helical Baffle Shell-and-Tube Heat Exchangers. Heat Transf Eng 2019. https://doi.org/10.1080/01457632.2019.1611135.

[61] Roosen P, Uhlenbruck S, Lucas K. Pareto optimization of a combined cycle power system as a decision support tool for trading off investment vs . operating costs. Int J Therm Sci 2003;42:553–60.

[62] Carapellucci R, Giordano L. A comparison between exergetic and economic criteria for optimizing the heat recovery steam generators of gas-steam power plants. Energy 2013;58:458–72. https://doi.org/10.1016/j.energy.2013.05.003.

[63] Uche J, Serra L, Valero A. Thermoeconomic analysis of a dual-purpose power and

desalination plant. Am Soc Mech Eng Adv Energy Syst Div AES 2000;40:201–9.

[64] Xiong J, Zhao H, Zhang C, Zheng C, Luh PB. Thermoeconomic operation optimization of a coal-fired power plant. Energy 2012;42:486–96. https://doi.org/10.1016/j.energy.2012.03.020.